

# Fluid-structure Interaction Analysis of Representative Left Coronary Artery Models with Different Angulations

Jingliang Dong<sup>1</sup>, Zhonghua Sun<sup>2</sup>, Kiao Inthavong<sup>1</sup>, Jiyuan Tu<sup>1</sup>

<sup>1</sup>School of Aerospace, Mechanical & Manufacturing Engineering, RMIT University, Melbourne, Australia

<sup>2</sup>Discipline of Medical Imaging, Department of Imaging and Applied Physics, Curtin University, Perth, Australia

## Abstract

*The aim of this study is to elucidate the correlation between coronary artery angulation and local mechanical forces at the vicinity of bifurcation using a coupled fluid-structure interaction (FSI) modelling approach. Four representative left coronary arteries with different angles ranging from 75° to 120° were used to demonstrate the relation between circumferential stress and angulation. In order to increase simulation fidelity, the arterial wall was modelled as an isotropic hyperelastic material, and physiologically reasonable waveforms were imposed at the boundaries. The results show that circumferential stress is positively correlated with left coronary artery angulation. In addition, the hemodynamic differences between the FSI modelling and rigid wall modelling was also addressed and analysed through comparing those two modelling techniques. The instantaneous wall shear stress (WSS) distributions were substantially affected by the arterial wall compliance.*

## 1. Introduction

Coronary heart disease is a major cause of death worldwide. It is believed that most important role in coronary heart disease is played by atherosclerosis caused by formation, developing, and rupture of plaques [1]. There is evidence implicating mechanical forces and intravascular hemodynamics resulting from blood flow (e.g. circumferential tensile stress and wall shear stress (WSS)) can chronically affect and regulate blood vessel structure in decades [2]. However, the complex etiology of atherosclerosis is not fully understood due to the unknown precise relationship between hemodynamics, mechanical factors and atherosclerotic changes of the arterial wall. Although a considerable connection between WSS and endothelial wall cells responses has been established [3], addressing these issues is always difficult since it is not yet possible to measure flow patterns and mechanical forces in vivo with a sufficient accuracy, even

with use of state of the art imaging techniques.

As shown in Figure 1, endothelial cells (ECs) in the vasculature experience two major hemodynamic forces in vivo, one is the fluid shear stress ( $\tau$ ), which is a frictional force imposed on per unit area from blood flow parallel to the vessel wall, and the other is the circumferential stress ( $P$ ), which is a normal force from transmural pressure [4]. Both fluid shear stress and circumferential stress play important roles in maintaining the homeostasis of the blood vessel, which also become pathophysiological factors in the complex pathogenesis of atherosclerosis [5, 6].

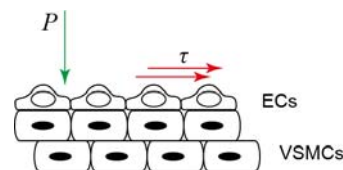


Figure 1. Hemodynamic forces imposed by the blood flow on the inner wall of artery vessel.

It is found that ECs are highly sensitive to shear stress, while vascular smooth muscle cells (VSMCs) appear mainly respond to circumferential stress [4]. It is also widely accepted that shear stress is negatively related to intima-media thickness (IMT) in healthy individuals [7]. In contrast, Carallo et al. [8] reported that circumferential stretch is positively correlated with IMT. Study of atherosclerosis is a complex disease associated with multiple factors, where early research was limited to analysis from a hemodynamic point of view are obviously not enough. Although Tang et al. [9] conducted a complex modelling of stenotic vessel segment, the effect of bifurcations was neglected.

The objective of the present study is to elucidate the correlation between coronary artery angulation and local mechanical forces (circumferential stress), which can contribute to the understanding of the pathogenesis of atherosclerosis at vicinity of bifurcations. To fulfil this

research objective, a series of parametric studies were conducted on the basis of four representative left coronary artery models (LCA) with different angles between its two main branches.

## 2. Methods

### 2.1. Vascular geometry reconstruction

As shown in Figure 2, a representative model was developed on the basis of 19 post-mortem casts of normal human coronary artery trees conducted by Nerem and Seed [10], which incorporates averaged anatomical data for vessel diameter, length and curvature. In order to reveal the effect of the angle variation, four representative models were constructed, and the angle ( $\alpha$ ) formed by left anterior descending branch (LAD) and left circumflex branch (LCx) was set into 75°, 90°, 105° and 120° respectively.

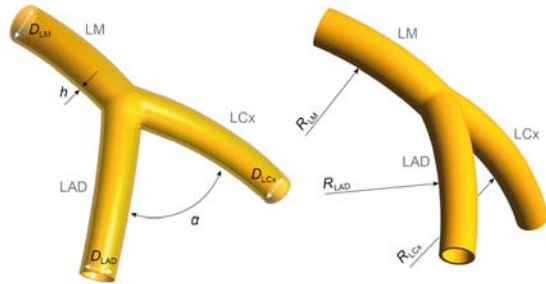


Figure 2. Geometry configuration of the representative model of human left coronary artery.

A constant wall thickness of 0.4 mm was assigned to the vessel walls [11], and other basic dimensions used in the construction of the representative model are listed in Table 1.

Table 1. Anatomical dimensions of the representative realistic model.

Length of LM	11.0 mm
Dia. of LM	4.0 mm
Dia. of LAD	3.4 mm
Dia. of LCx	3.0 mm
Rad. of curvature of LAD	42.8 mm
Rad. of curvature of LCx	39.3 mm

### 2.2. Model parameters

Although arterial wall is known to be a composite tissue including collagen fibers, its heterogeneous and anisotropic structure properties was simplified by adopting a nine parameter Mooney-Rivlin hyperelastic

model due to lack of in vivo data [12]. Detailed model parameters were set following the FSI analysis of human right coronary artery conducted by Koshiba et al. [13]. The blood was assumed to be Newtonian fluid since it was widely accepted that the shear rate is consequently large enough in coronary arteries (larger than  $100 \text{ s}^{-1}$ ) to maintain a flow regime with nearly constant viscosity [14]. The density and viscosity of the blood used in this study were set as  $1060 \text{ kg/m}^3$  and  $0.0035 \text{ Pa}\cdot\text{s}$ . Physiological reasonable flow waveforms [15] employed in this study are shown in Figure 3, and blood flow was treated as laminar.

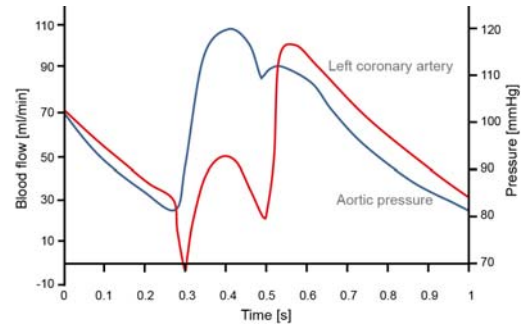


Figure 3. Cardiac pulsatile velocity and pressure profiles.

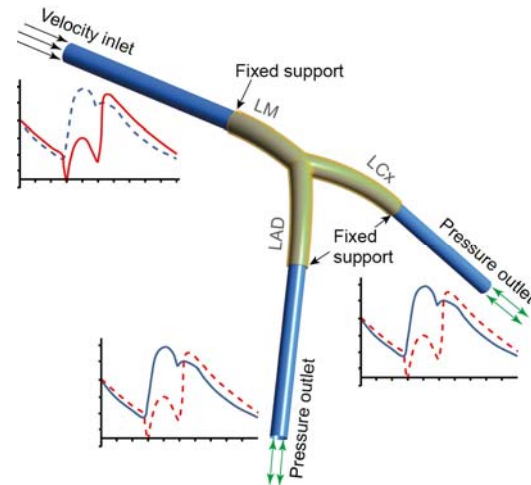


Figure 4. Boundary setup for FSI and rigid wall modelling methods.

As shown in Figure 4, fixed support was applied to each model at the inlet and outlets and no axial or transaxial motion was permitted. Both FSI and rigid wall models were performed under the same inlet and outlet boundary conditions, no-slip wall boundary condition was imposed at the internal surface of the bifurcation, while for FSI simulation, it also serves as the fluid-solid interface. Flow extensions of ten times its diameter (10D) were added to generate fully developed flow and avoid any back flow at outlets (Figure 4).

### 3. Results

Both rigid wall and FSI simulation were successfully performed using commercial software package ANSYS-CFX, and the hemodynamic difference between rigid and compliant models were addressed. Furthermore, mechanical force analysis was also provided in this section. Both demonstrate that vessel compliance can affect blood flow patterns considerably and plays important role in the pathogenesis of atherosclerosis.

#### 3.1. WSS analysis

As shown in Figure 5, analysis of WSS was focused on low shear stress value, as it was reported that low shear stress was positively related to intima-media thickness (IMT) in healthy individuals.

Generally, low shear stress region is concentrated at origins of LAD and LCx branches, and LCx experiences a larger low shear stress area than that of LAD. Meanwhile, low shear stress region is found to reduce when the branch angle increases.

The effect of wall compliance on instantaneous WSS distribution is also shown in Figure 5, where similar but quantitatively different WSS distributions are established for rigid wall and FSI models. At the peak of a cardiac cycle, WSS for the FSI model is lower than that in the rigid wall model, and this difference is more obvious in the proximal of LAD branch. This is mainly due to the artery vessel deformation driven by pulsatile blood flow. As a consequence, flow disturbance is weakened and velocity at the near wall region increases. Finally, low WSS region are more prominent in the rigid wall model on the LAD side in comparison with FSI model.

#### 3.2. Mechanical force analysis

Both mechanical deformation in the form of total mesh displacement and stress distribution are presented in Figure 6. Vessel deformation occurs at the bifurcation region, and it expands downstream as the branch angle increases. Conversely, the intensity of the deformation decreases when the branch angle becomes larger.

First principal stress is used for stress distribution analysis, as it represents the maximum tensile stress included in the vessel wall due to the pulsatile loading of blood flow. Large first principal stress value occurs at junction area formed by the left main stem and those two main branches, and the maximum value happens at the apex of the bifurcation. In addition, the principal stress value at out-wall of the junction area increases in wide-angled models, while it decreases at the apex of the bifurcation.

Therefore, the focally concentrated first principal stress may contribute to induce atherosclerosis at this

region, or result to plaque rupture if a vulnerable plaque also exists in this district.

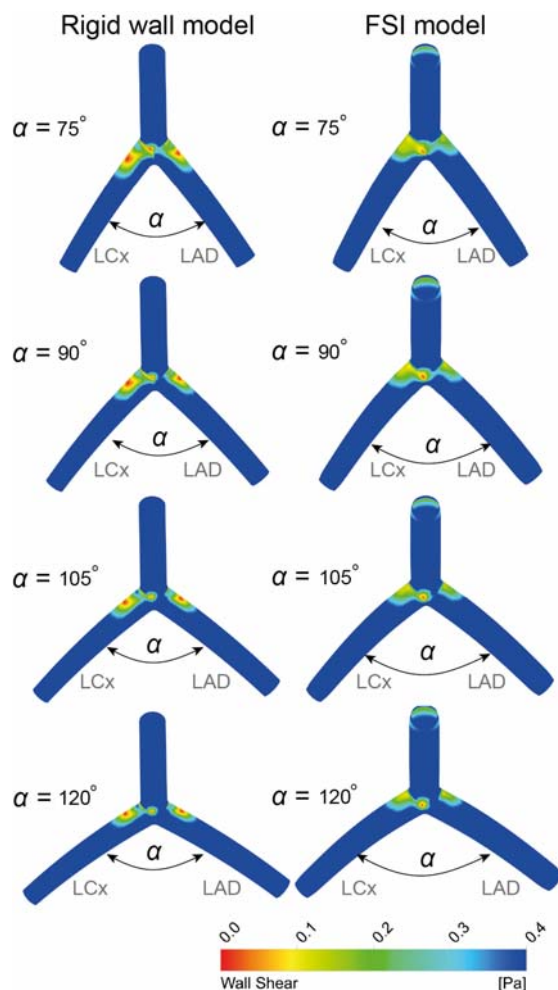


Figure 5. WSS distribution at peak systolic phase of rigid wall and FSI modelling.

### 4. Conclusion

In addition to the conventional rigid wall modelling, FSI simulations were performed in this paper. On the basis of rigid wall and FSI simulation results, direct relationships between branch angulation and hemodynamic and mechanical changes are sorted out.

In order to simplify the model and analysis, some limitations in this paper should be addressed. Firstly, fixed supports both on inlet and outlets restrict further deformation of the vessel. Secondly, only the peak events are selected for results discussion, which also limits the robustness of our conclusion.

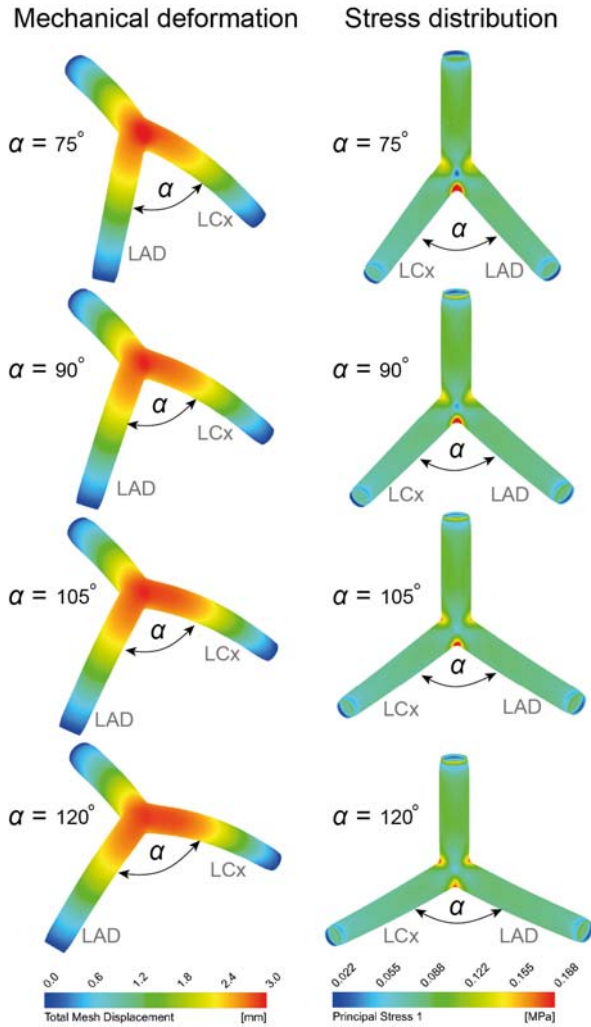


Figure 6. Deformation and stress distribution at peak systolic phase.

## Acknowledgements

The authors acknowledge financial support provided by the Australian Research Council (ARC project ID DP0986183), and Jingliang Dong also especially thanks for the scholarship provided by China Scholarship Council (CSC Student ID 2010608027) and RMIT University.

## References

- [1] Ohayon J, et al. Necrotic core thickness and positive arterial remodeling index: emergent biomechanical factors for evaluating the risk of plaque rupture. *American journal of physiology-heart and circulatory physiology* 2008; 295: H717-727.
- [2] Slager CJ, et al. The role of shear stress in the destabilization of vulnerable plaques and related therapeutic implications. *Nature clinical practice,*

*cardiovascular medicine* 2005; 2: 456-464.

- [3] Stone PH, et al. Regions of low endothelial shear stress are the sites where coronary plaque progresses and vascular remodelling occurs in humans: an in vivo serial study. *European heart journal* 2007; 28: 705-710.
- [4] Hahn C, Schwartz MA. The role of cellular adaptation to mechanical forces in atherosclerosis. *Arteriosclerosis, thrombosis, and vascular biology* 2008; 28: 2101-2107.
- [5] Chien S, Li S, Shyy YJ. Effects of mechanical forces on signal transduction and gene expression in endothelial cells. *Hypertension* 1998; 31: 162-169.
- [6] Lehoux S, Tedgui A. Signal transduction of mechanical stresses in the vascular wall. *Hypertension* 1998; 32: 338-345.
- [7] Gnasso A, et al, Association between intima-media thickness and wall shear stress in common carotid arteries in healthy male subjects. *Circulation*, 1996. 94: 3257-3262.
- [8] Carallo C, et al. Evaluation of common carotid hemodynamic forces. Relations with wall thickening. *Hypertension* 1999; 34: 217-221.
- [9] Tang D, et al. 3D MRI-based anisotropic FSI models with cyclic bending for human coronary atherosclerotic plaque mechanical analysis. *Journal of biomechanical engineering* 2009; 131: 061010.
- [10] Nerem RM, Seed WA. Coronary artery geometry and its fluid mechanical implications, in *Fluid dynamics as a localizing factor for atherosclerosis*, Schettler G, Editor 1983, Springer-Verlag Press., 51-59.
- [11] Colombo A, et al. A method to develop mock arteries suitable for cell seeding and in-vitro cell culture experiments. *Journal of the mechanical behavior of biomedical materials* 2010; 3: 470-477.
- [12] Torii R, et al. Fluid-structure interaction analysis of a patient-specific right coronary artery with physiological velocity and pressure waveforms. *Communications in numerical methods in engineering* 2009; 25: 565-580.
- [13] Koshiha N, et al. Multiphysics simulation of blood flow and LDL transport in a porohyperelastic arterial wall model. *Journal of biomechanical engineering* 2007; 129: 374-385.
- [14] Gijssen FJ, et al. A new imaging technique to study 3-D plaque and shear stress distribution in human coronary artery bifurcations in vivo. *Journal of biomechanics* 2007; 40: 2349-2357.
- [15] Chaichana T, Sun Z, Jewkes J. Computation of hemodynamics in the left coronary artery with variable angulations. *Journal of biomechanics* 2011; 44: 1869-1878.

Address for correspondence.

Prof. Jiyuan Tu  
 School of Aerospace, Mechanical and Manufacturing Engineering, RMIT University, VIC 3083, Australia  
 jiyuan.tu@rmit.edu.au  
 Phone: +61-3-9925-6191;  
 Fax: +61-3-9925-6108.